Universidad de Concepción
Dirección de Postgrado
Facultad de Ingeniería - Programa de Magister en Ciencias de la Ingeniería con mención en Ingeniería Civil

CHILEAN LIQUEFACTION DATABASE

(BASE DE DATOS CHILENA DE LICUACIÓN)

Tesis para optar al grado de Magíster en Ciencias de la Ingeniería con Mención en Ingeniería Civil

DANIELA PAZ ESPINOZA PULGAR
CONCEPCIÓN - CHILE
2021

Profesor Guía: Dr. Gonzalo Montalva Alvarado
Dpto. de Ingeniería Civil, Facultad de Ingeniería
Universidad de Concepción

ABSTRACT

This research describes a liquefaction database that contains a summary of 209 liquefaction, non-liquefaction and marginal case histories compiled from 2010 Mw 8.8 Maule, 2014 Mw 8.2 Iquique, 2015 Mw 8.3 Illapel, and 2016 Mw 7.6 Melinka seismic events, where the liquefaction phenomenon caused damage to buildings, bridges, roads, and drainage systems, generating millions in losses at the infrastructure level. The database structure is organized into three main tables defined as site information, geotechnical tests, and seismic parameters. The main tables include the location of the sites, surface evidence of liquefaction or the absence of them, geotechnical parameters from boreholes, geophysical and laboratory tests. In addition, seismic parameters of these seismic events are included as well as also ground motion intensity measures estimated for the sites. Intensity measures included are peak ground acceleration and velocity, pseudo-spectral horizontal acceleration and Housner intensity. The information in this database will allow a better characterization of the seismic demand and the geotechnical properties of the soil involved in the prediction of liquefaction triggering. The data associated with this article are available in DesignSafe (https: // XXXXX), where users can freely download and process data, to train or evaluate predictive liquefaction models.

ACKNOWLEDGEMENTS

This work was partially funded by the National Commission for Scientific and Technological Research (CONICYT) through the projects FONDEF IDeA 16I1015 and FONDEF ID16i20157, this support is greatly acknowledged.

The author thanks the Roads Department of the Ministry of Public Works (MOP) for providing essential data for the development of this work. Thanks Engineer Francisco Ruz who is also part of the project through associated company Ruz & Vukasovic Engineers.

Thanks Dr. Gonzalo Montalva for the support in the development of the thesis. In addition, special thanks go to the geotechnical research group at University of Concepción for the fieldwork performed to collect and process data.

Finally, the author thanks her family, boyfriend, and friends for the unconditional love and support provided during the development of this research.

CONTENTS

LIST OF TABLES

LIST OF FIGURES

CHAPTER 1 INTRODUCTION

1.1 Motivation

For the last 50 years the semi- empirical procedures have evolved as a standard of practice to evaluate the liquefaction triggering in soils. The development of this procedures consists in a relation between the seismic demand of the soil layer, and the capacity of the soil to resist liquefaction. Seismic demand, or Cyclic Stress Ratio (CSR), it is defined as a function of the shear stress induced by the earthquake and incorporates an acceleration and magnitude estimated from a seismic risk analysis or chosen deterministically. The capacity of the soil to resist liquefaction (CRR) is expressed in terms of soil resistance, which can be obtained through standard penetration test (SPT), cone penetration tests (CPT), shear wave velocity measurement (Vs) and Becker penetration test (BPT). Recent updates to these procedures include Youd et al. (2001), Cetin et al. (2004) (2018) and Idriss and Boulanger (2010) (SPT procedures); Boulanger and Idriss (2016) (CPT procedure); Andrus and Stokoe (2000), Kayen et al. (2013) and Dobry and Abdoun (2015) (Vs procedures). It should be noted that these procedures predict the occurrence of liquefaction in the most critical layer of a site, and not predict if surface manifestation there will be.

Chile is one of the countries with the highest seismic activity in the world. Chilean seismic records show the phenomenon of liquefaction throughout it is history, as could be seen in the effects of the 1960 Mw 9.5 Valdivia earthquake (Pastén, et al., 2021). Recently four large earthquakes occurred in Chile: the 2010 Mw 8.8 Maule, 2014 Mw 8.2 Iquique, 2015 Mw 8.3 Illapel and 2016 Mw 7.6 Melinka, where the liquefaction phenomenon caused multiple damages generating millions in losses at the infrastructure level.

The procedures found in the literature to estimate the potential of liquefaction in Chile, present an important dispersion of data and errors in the prediction of the phenomenon. This has been exposed in the first instance by (Montalva & Leyton, 2014). Subsequently, Montalva and Ruz (2017) evaluated the resistance to liquefaction of a Chilean database made up of thirty sites, using standard penetration test (SPT) and shear wave velocity (Vs)

procedures. The error of each procedure was defined as the percentage of sites where the occurrence of liquefaction was not correctly predicted, and the procedures presented errors higher than 36,7% in the prediction of the phenomenon in Chile. From these results arises the need to create, systematize and implement a national database of free access to achieve a better analysis and prediction of liquefaction triggering.

To address the objective of this research, 209 liquefaction, non-liquefaction and marginal case histories were compiled from the seismic events of 2010 Mw 8.8 Maule, 2014 Mw 8.2 Iquique, 2015 Mw 8.3 Illapel and 2016 Mw 7.6 Melinka. Case history data was acquired from technical publications in the form of articles, engineering and/or site reconnaissance reports and undergraduate research from Chilean universities. After that, the database was expanded and corrected with geotechnical, geophysical and laboratory test data. This information was obtained through reports of soil mechanics, scientific articles, and fieldwork from the geotechnical group of the University of Concepción. Finally, seismic parameters of the seismic events were incorporated as well as also ground motion intensity measures estimated for the sites.

The data associated with this research are available in DesignSafe (https: // XXXXX), where users can freely download and process data, to train or evaluate predictive liquefaction models.

1.2 Hypothesis

The working hypothesis for this research is the following: “The creation and implementation of a national free access database, will allow a better characterization and estimation of the liquefaction triggering in subduction zones”.

1.3 Objectives

1.3.1 General Objective

The general objective is to create, systematize and implement a free access Chilean liquefaction database.

1.3.2 Specific Objectives

- Compile liquefaction, non-liquefaction, and marginal case-histories from the seismic events of 2010 Mw 8.8 Maule, 2014 Mw 8.2 Iquique, 2015 Mw 8.3 Illapel, and 2016 Mw 7.6 Melinka.
- Characterize the seismic and geotechnical parameters used to predict the occurrence of liquefaction.
- Generate and implement a database structure with the compiled information.
- Analyze the available data quantitatively and qualitatively.

1.4 Methodology

To address the objectives of this research, the methodology was divided into four stages:

- A complete review of the state of art of liquefaction phenomenon in Chile and the world was realized, with major emphasis in the methodologies used to predict liquefaction triggering and the soil parameters involved.
- Liquefaction, non-liquefaction, and marginal case-histories were compiled from the seismic events 2010 Maule, 2014 Iquique, 2015 Illapel and 2016. After that, geotechnical, geophysical and laboratory test data were incorporated. Finally, seismic parameters of the seismic events were incorporated as well as also ground motion intensity measures estimated for the sites.
- A relational database was created, incorporating the seismic and geotechnical parameters from the case history data.
- A qualitative and quantitative analysis of the parameters involved in the phenomenon was realized to finally present the results obtained.

1.5 Main results and conclusions

A Chilean liquefaction database was created to characterize the seismic and geotechnical parameters used to predict the occurrence of liquefaction. For this purpose, 209 liquefaction,

non-liquefaction and marginal case histories were compiled from seismic events of 2010 Mw 8.8 Maule, 2014 Mw 8.2 Iquique, 2015 Mw 8.3 Illapel and 2016 Mw 7.6 Melinka. It is included a description of the database structure, followed by the historical performance (surface evidence), geotechnical, geophysical and laboratory test data, earthquake information and ground motion intensity measures

The data associated with this research are available in DesignSafe (https: // XXXXX), where users can freely download and process data, to train or evaluate predictive liquefaction models.

The information gathered and reported in this database should serve as a tool to achieve a better characterization of seismic demand and geotechnical properties of soil, which will allow a better analysis of the variables involved in the liquefaction phenomenon and can be helpful in several engineering applications nationwide.

1.6 Thesis structure

Chapter 1 presents the general problem to be investigated, working hypothesis, and general and specific objectives, as well as an outline of the methodology. Chapter 2 present a review of the state of art of liquefaction phenomenon in Chile and the world, with major emphasis in the methodologies used to predict liquefaction triggering and the soil parameters involved. Chapter 3 describes the materials and methods, in particular the structure of the database and the information compiled to characterize the parameters involved in the occurrence of liquefaction. Chapter 4 presents the main results of the investigation. Finally, Chapter 5 concludes with final remarks on the obtained results and ways to proceed forward.

CHAPTER 2 STATE OF ARTS REVIEW

2.1 Introduction

Soil liquefaction is a phenomenon that has been widely studied over the last 50 years, due to the severe damage it can cause not only to the soil, but also to structures. For this reason, different authors propose procedures to predict the occurrence of liquefaction, which were calibrated using data from field measurements and laboratory tests. This chapter presents a brief literature review on the main effects of soil liquefaction and the soil parameters involved in this phenomenon.

2.2 Phenomenon of liquefaction

Soil dynamics includes the phenomenon of liquefaction, a term that is associated with the loss of rigidity and/or resistance of sandy soils in a saturated state. Liquefaction is the natural process in which soils lose part of their mechanical strength in response to cyclical dynamic loads such as an earthquake. This loss of resistance causes the soil to behave momentarily in a similar way to a fluid, which can generate significant deformations in the soil.

Liquefaction is generated mainly in loose and saturated granular soils, which are usually located near riverbanks, coastal edges, near bodies of water, or have a very shallow water table. In addition, it occurs in soils that have low compaction, such as the grounds located in areas where lakes, lagoons and wetlands previously existed.

The soils most susceptible to this phenomenon are saturated granular materials with a poor degree of densification and medium drainage capacity, such as sandy silts and poorly graded sands. Liquefaction induces a significant level of deformation, causing permanent settlements and damage to structures founded on these materials. In soils with low slopes and adjacent to rivers, a displacement occurs that generates lateral spreading faults. Additionally,

the increase in interstitial pressures causes eruptions of soil and water, which are evident on the surface in the form of sand boils.

The tendency of the dry non-cohesive soils to densify under static and cyclical loads is well known. However, when non-cohesive soils are saturated and expose to an earthquake, the cyclic loading occurs under non-draining conditions, so the tendency to densification increases excess pore pressure and decreases effective stress, which causes any structure founded on the ground to sink or suffer differential (Kramer, 1996).

The liquefaction study began in 1964 after the earthquakes in Alaska and Niigata in Japan, because the damage caused to the structures was not structural and the damage to the soil could not be explained with the geotechnical studies developed up to that time.

The study of liquefaction began in 1964 after the earthquakes in Alaska and Niigata in Japan, because the damage caused to the structures was not structural and the damage to the soil could not be explained with the geotechnical studies developed until that moment. The first analyzes were focus on the use of in-situ tests, mainly in Standard Penetration Tests (SPT), and as a consequence of these, the first methodologies were obtained to estimate the soil liquefaction potential, principally the proposed by Seed & Idriss (1971).

2.3 Evaluation of the soil liquefaction potential

For the last 50 years the semi- empirical procedures have evolved as a standard of practice to evaluate the liquefaction triggering in soils. The development of this procedures consists in a relation between the seismic demand of the soil layer, and the capacity of the soil to resist liquefaction. Seismic demand, or Cyclic Stress Ratio (CSR), it is defined as a function of the shear stress induced by the earthquake and incorporates an acceleration and magnitude estimated from a seismic risk analysis or chosen deterministically. Figure 1 shows the scheme to estimate the demand or Cyclic Stress Ratio, CSR.

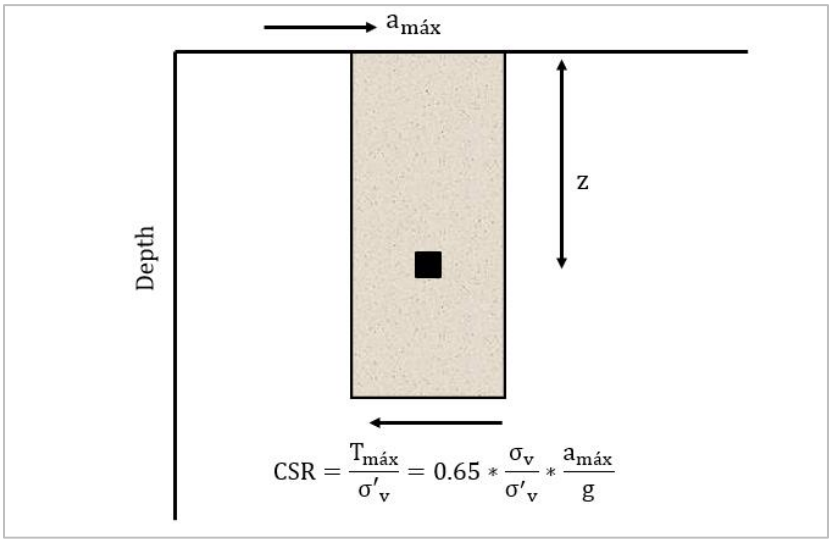

Figure 1 Scheme to estimate the demand or Cyclic Stress Ratio, CSR

The capacity of the soil to resist liquefaction (CRR) is expressed in terms of soil resistance, which can be obtained through standard penetration test (SPT), cone penetration tests (CPT), shear wave velocity measurement (Vs) and Becker penetration test (BPT).

The procedure proposed by Seed & Idriss (1971) is the basis for most of the methodologies used today and proposes the estimation of a Safety Factor (FS) at the occurrence of liquefaction, which corresponds to the ratio between the probable site demand (CSR), and the demand required to trigger liquefaction, given the properties of the soil. This required demand is called CRR (Cyclic Resistance Ratio) and corresponds to the curve that separates the sites susceptible to liquefaction from those that should not liquefy. In the last 45 years, numerous authors have made considerable improvements to this method, increasing and refining the database, calibrating factors, and introducing new capacity parameters.

Recent updates to these procedures include Youd et al. (2001), Cetin et al. (2004) (2018) and Idriss and Boulanger (2010) (SPT procedures); Boulanger and Idriss (2016) (CPT procedure); Andrus and Stokoe (2000), Kayen et al. (2013) and Dobry and Abdoun (2015) (Vs procedures). It should be noted that these procedures predict the occurrence of liquefaction in the most critical layer of a site, and not predict if surface manifestation there will be.

2.4 Liquefaction in Chile

Chile is one of the countries with the highest seismic activity in the world. Chilean seismic records show the phenomenon of liquefaction throughout it is history, as could be seen in the effects of the 1960 Mw 9.5 Valdivia earthquake (Pastén, et al., 2021). Recently four large earthquakes occurred in Chile: 2010 Maule, 2014 Iquique, 2015 Illapel and 2016 Melinka, where the liquefaction phenomenon caused multiple damages generating millions in losses at the infrastructure level. The Figure **2** shows the effects of liquefaction in Chilean soils after the seismic events previously mentioned.

Figure 2 Effects of liquefaction phenomenon after the four large earthquakes occurred in Chile. Top left: Mataquito Bridge (Maule 2010); top right: Huara Bridge (Iquique 2014); bottom left: Lighthouse/El Faro of La Serena (Illapel 2014); bottom right: flow failure in Puqueldón (Melinka 2016).

The procedures found in the literature to estimate the potential of liquefaction in Chile, present an important dispersion of data and errors in the prediction of the phenomenon. This has been exposed in the first instance by (Montalva & Leyton, 2014). Subsequently, Montalva and Ruz (2017) evaluated the resistance to liquefaction of a Chilean database made up of thirty sites, using standard penetration test (SPT) and shear wave velocity (Vs) procedures. The error of each procedure was defined as the percentage of sites where the occurrence of liquefaction was not correctly predicted, the results of each methodology are shown in the Table 1. From these results arises the need to create, systematize and implement a national database of free access to achieve a better analysis and prediction of liquefaction in Chilean soils.

Table 1 Errors for each methodology (Montalva & Ruz, 2017)

Methodology	**Error**
Youd et al. 2001	36.7%
Cetin et al. 2004	43.3%
Idriss & Boulanger 2008	43.3%
Andrus & Stokoe 2000	43.3%
Kayen et al. 2013	46.0%
Dobry & Abdoun 2015	57.1%

2.5 Conclusion

This chapter presents the basic theory to understand the liquefaction phenomenon and its relevance in geotechnical engineering. In addition, the state of the art is presented at national level, evidencing the limited success of existing procedures to predict the liquefaction triggering in Chilean soils.

CHAPTER 3 MATERIALS AND METHODS

3.1 Introduction

An important part in the development of predictive models of liquefaction is having a database that provides the highest possible productivity and accuracy to subsequent analyzes. This chapter begins with the presentation of the database structure, followed by the historical performance (surface evidence of liquefaction) of the case-history data, and how these were selected, to finally explain the geotechnical and seismic properties incorporated in the database.

3.2 Database Structure

The database presented herein follows the work by Cetin et al (2018) and NGL (Brandenberg, Zimmaro, & Stewart, 2020) and corresponds to a relational database. This type of database is based on the relational model, a straightforward way to organize data in tables. In a relational database, data is organized as a set of tables with columns and rows, where each row in the table is a record with a unique ID called a key and each column contains the attributes of the data, making the relationships between the data points easy to find.

The database structure is organized into three main tables defined as site information [SITE], geotechnical tests [TEST], and seismic parameters [SPAR]. A site represents a homogeneous geographic area on the ground surface, with observations of surface manifestations of liquefaction after seismic events and presenting relevant field data. Site information tables are subdivided into site background [SITE_SBGND] and evidence of liquefaction [SITE_LE] (Figure 3). Site backgrounds tables contain the site identification (site ID), latitude and longitude (degrees, minutes and seconds), location city and region, structure type (i.e., building, bridge, free-field level ground) and geological age. Evidence of liquefaction table contain the classification of site performance during the earthquake classified as "surface manifestations of liquefaction", "no visible surface manifestations of liquefaction",

or "marginal" and tables to describe the surface evidence of liquefaction which are divided into photographs and field commentaries. It is important to note that minimum data requirements for the site information table are location city, latitude and longitude and site performance.

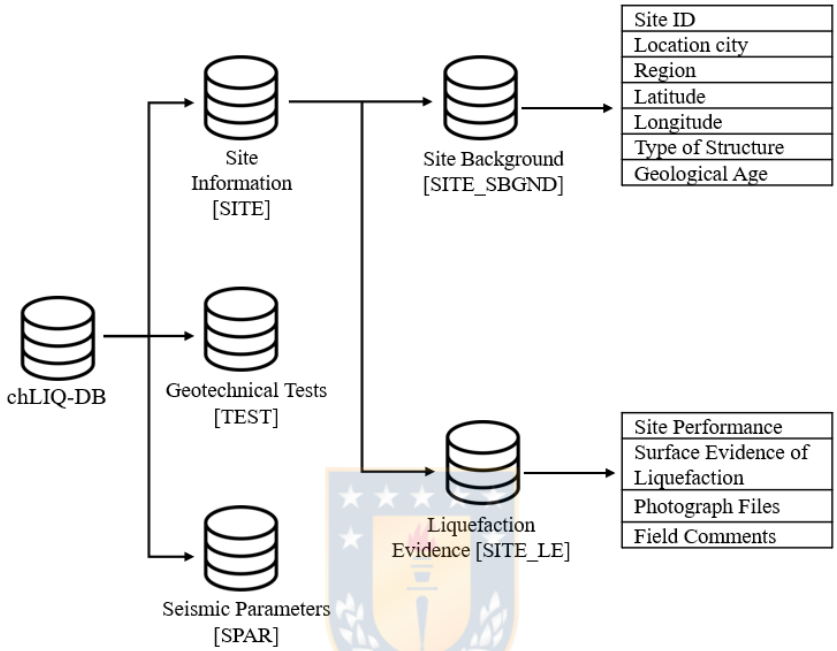

Figure 3. Relational schema illustrating the three main tables of the data structure and the tables containing the site background and evidence of the liquefaction data.

The geotechnical tests tables [TEST] contain information from SPT data [TEST_SPT], geophysical measurements [TEST_SWG], predominant frequency [TEST_PFREQ], and CPT data [TEST_CPT] (Figure 3). SPT data tables contains the total quantity of boreholes realized in the site and incorporates tables with the latitude and longitude of the test, groundwater table depth, hammer energy, bar diameter and soil layers. The soil layer tables contain SPT blow count (N_m) and laboratory test data from samples obtained in the boreholes. Database incorporates tables with particle size distribution (sieves #4, #10, #40 and #200), Atterberg limits (liquid limit, plastic limit, and plasticity index), USCS classification, moisture content and specific gravity (Gs). The geophysical measurements tables contain geophysical test data obtained from measurements at the study sites and incorporates tables with dispersion curve of the phase velocity of Rayleigh waves, shear wave velocity profile

(V_s) and average shear wave velocity to a depth of 18 and 30 meters (V_{s18}; V_{s30}). Predominant frequency tables incorporate latitude and longitude of the instrument (degrees, minutes, and seconds), duration of the records, HVSR curves (H/V predominant frequency and amplitude) and if is a clear peak (yes or no). CPT data tables contains the total quantity of boreholes realized in the site and incorporates tables with the latitude and longitude of the test (degrees, minutes, and seconds), ground water table, tip resistance, sleeve friction, pore pressure and cone resistance.

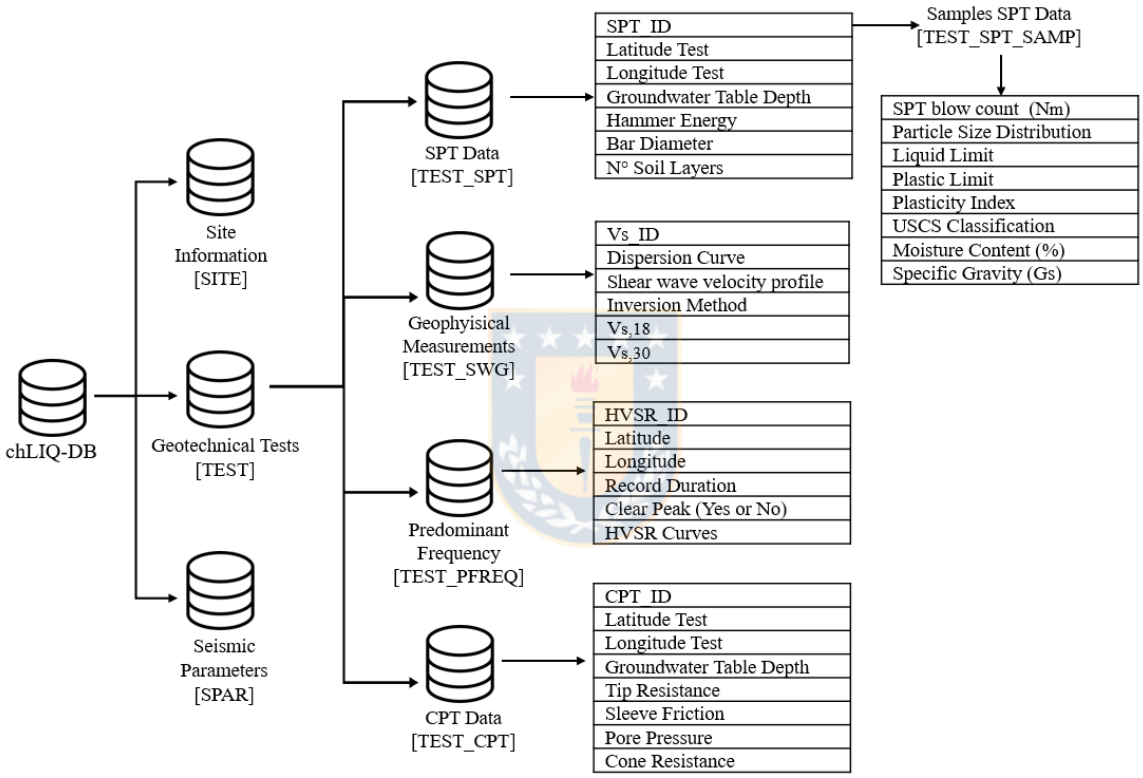

Figure 4. Relational schema illustrating the geotechnical test tables and the tables containing the SPT data, geophysical measurements data, predominant frequency and CPT data.

The seismic parameters tables [SPAR] contain information from seismic events [SPAR_SEVENT] and ground motion intensity measures [SPAR_IM] (Figure 4). Seismic events tables contain the event name, event date, event magnitude, hypocenter locations (latitude, longitude, and depth), seismogenesis of the event, closest distance, epicentral distance, and hypocentral distances. The intensity measures tables included in the database

are the peak ground acceleration and velocity, pseudo-spectral horizontal accelerations (PSA), spectral velocities (SV) and Housner intensity (I_H).

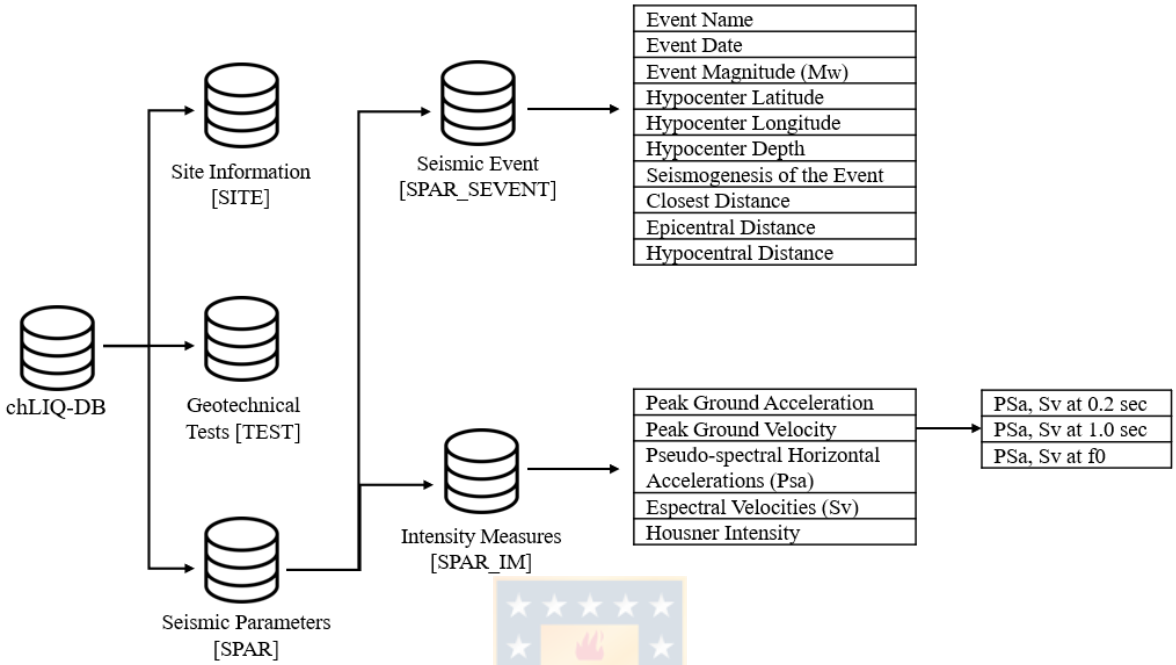

Figure 5. Relational schema illustrating the seismic parameters tables and the tables containing the seismic events and intensity measures data.

3.3 Site Performance

In analytical and field work it is important to make the distinction between the occurrence of liquefaction and the observation of the surface manifestations of liquefaction. While the first can occur without the second, the second cannot occur without the first.

Site performance during seismic events was classified as liquefaction, no liquefaction, and marginal liquefaction. In the compiled of the cases histories, the site performance was based on the classification assigned by the original investigator. Subsequently, following the work done by Boulanger and Idriss (2014), all original sources were analyzed and discussed to obtain interpretations consistent with our current understanding and knowledge.

Sites with evidence of liquefaction correspond all the areas that presented damages an observations of liquefaction effects after seismic events and were accompanied with reports of visible ground failures and deformations in the form of excessive settlement, lateral spreading, sand boils, surface cracks, flow failures, etc. This does not rule out that there are numerous sites that developed this phenomenon in depth and did not appear on the surface. Sites described as non-liquefaction were either accompanied with reports of no visible surface manifestations (i.e., no sand boils, ground surface settlements, or lateral spreading) or can be inferred as having corresponded to such conditions when not explicitly stated.

The sites described as marginal correspond to all areas close to sites with evidence of liquefaction, but without surface evidence. Therefore, they are probably near to the borderline behavior between the manifestation of superficial liquefaction and the absence of it. These sites are particularly useful for the purpose of the research.

Case history data was acquired from technical publications in the form of articles, engineering and/or site reconnaissance reports (Yasuda, et al., 2010); (FHWA, 2011); (González & Verdugo, 2014); and (Montalva & Leyton, 2014), reports from the National Geology Service and Mining (Sernageomin, 2010) and (Sernageomin, 2017), reports from the Geotechnical Extreme Events Reconnaissance association (GEER, 2010); (GEER, 2014); and (GEER, 2015), undergraduate research from Chilean universities (Contreras, 2012), (Alfaro, 2013); (González, 2015); (Roncagliolo, 2017); and (Espinoza, 2018), reports from the Ministry of Public Works (MOP) and the fieldwork of the University of Concepción in Illapel 2015.

The database spans an approximate distance of 2800 km from Arica to Chiloé, and the main evidence of liquefaction were found in the south of the country, which is explained by the predominance of sandy soils and the major presence of rivers, lakes, and aquifers shallow, which differs with the characteristics of the soil located in the north-central part of the country. The surface manifestations, or the absence of them, were classified according to ground failures or type of structures affected in the following groups:

1. Sand boils
2. Lateral spreading
3. Flow Failure
4. Excessive settlement
5. Structure Flotation
6. Surface Cracks
7. Structure Damage
8. Buildings
9. Bridges and overpasses
10. Free-field level ground
11. Roads and drainage systems
12. Tailing dams

Given the above, the term liquefaction will be used to describe the surface manifestations of liquefaction. Also, sites could be classified in more than one category, so these classifications are not exclusive.

3.4 Seismic Events

The database presented herein includes 121 liquefaction, 82 non-liquefaction, and 6 marginal liquefaction case histories from 2010 Mw 8.8 Maule, 2014 Mw 8.2 Iquique, 2015 Mw 8.3 Illapel, and 2016 Mw 7.6 Melinka seismic events. As shown in Figure 6, the principal case histories correspond to Maule 2010.

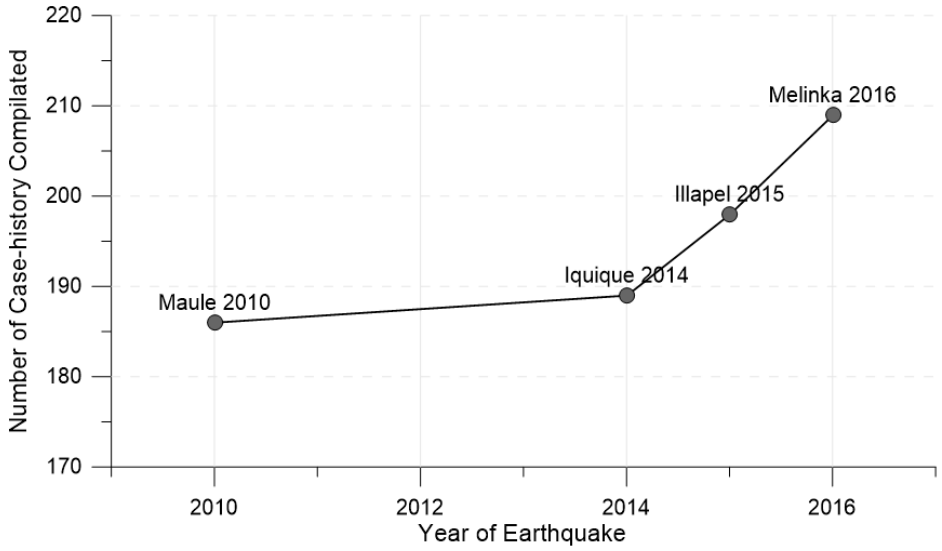

Figure 6. Cumulative case-history data compiled

3.5 Geographic Location

The Table 2 shows the 209 sites that compose the database, including latitude and longitude (degrees, minutes, and seconds), location city, seismic event associated, and the classification of site performance during the earthquake. It is important to mention that these sites are not an exhaustive sample of all the sites that were identified after the earthquakes.

Table 2 Case histories database

Site_ID	City Location	Latitude	Longitude	Seismic Event	Surface Evidence of Liquefaction
01	Concepción	-36.8056	-73.0222	2010 Mw 8.8 Maule	No
02	Concepción	-36.8180	-72.9890	2010 Mw 8.8 Maule	No
03	Concepción	-36.7859	-73.0380	2010 Mw 8.8 Maule	No
04	Concepción	-36.7898	-73.0636	2010 Mw 8.8 Maule	No
05	Concepción	-36.7910	-73.0576	2010 Mw 8.8 Maule	No
06	Concepción	-36.8193	-73.0620	2010 Mw 8.8 Maule	No
07	San Pedro de La Paz	-36.8429	-73.1071	2010 Mw 8.8 Maule	No
08	Valdivia	-39.8348	-73.2548	2010 Mw 8.8 Maule	No
09	Los Ángeles	-37.4710	-72.3507	2010 Mw 8.8 Maule	No
10	Los Ángeles	-37.4697	-72.3514	2010 Mw 8.8 Maule	No
11	Arauco	-37.2469	-73.3168	2010 Mw 8.8 Maule	Yes
12	Arauco	-37.2464	-73.3209	2010 Mw 8.8 Maule	Yes
13	Los Ángeles	-37.4834	-72.3713	2010 Mw 8.8 Maule	Yes
14	Constitución	-35.3308	-72.4123	2010 Mw 8.8 Maule	No
15	Constitución	-35.3354	-72.4043	2010 Mw 8.8 Maule	No
16	Constitución	-35.3336	-72.4071	2010 Mw 8.8 Maule	No
17	Valparaíso	-33.5748	-71.6271	2010 Mw 8.8 Maule	No
18	Valparaiso	-33.0427	-71.6084	2010 Mw 8.8 Maule	No
19	Concepción	-36.8151	-73.0468	2010 Mw 8.8 Maule	Yes
20	Concepción	-36.8301	-73.0680	2010 Mw 8.8 Maule	Yes
21	Concepción	-36.8159	-73.0837	2010 Mw 8.8 Maule	Yes
22	Concepción	-36.7909	-73.0813	2010 Mw 8.8 Maule	Yes
23	Coronel	-37.0276	-73.1500	2010 Mw 8.8 Maule	Yes
24	La Serena	-29.8971	-71.2686	2015 Mw 8.3 Illapel	No
25	La Serena	-29.9054	-71.2741	2015 Mw 8.3 Illapel	Yes
26	Paine	-33.8699	-70.7264	2010 Mw 8.8 Maule	Yes
27	Paine	-33.8613	-70.7459	2010 Mw 8.8 Maule	Yes
28	Valparaiso	-33.0450	-71.6194	2010 Mw 8.8 Maule	No
29	Concepción	-36.8371	-73.0629	2010 Mw 8.8 Maule	Yes

Site_ID	City Location	Latitude	Longitude	Seismic Event	Surface Evidence of Liquefaction
30	Chiguayante	-37.1681	-72.8977	2010 Mw 8.8 Maule	Yes
31	Coelemu	-36.4797	-72.7041	2010 Mw 8.8 Maule	Marginal
32	Dichato	-36.5451	-72.9325	2010 Mw 8.8 Maule	Marginal
33	Coelemu	-36.4670	-72.6932	2010 Mw 8.8 Maule	Yes
34	Laraquete	-37.1666	-73.1844	2010 Mw 8.8 Maule	Marginal
35	Arauco	-37.2545	-73.4366	2010 Mw 8.8 Maule	Yes
36	Coronel	-37.0297	-73.1459	2010 Mw 8.8 Maule	No
37	Talcahuano	-36.7819	-73.0887	2010 Mw 8.8 Maule	No
38	Concepción	-36.7840	-73.0451	2010 Mw 8.8 Maule	No
39	Chiguayante	-36.9506	-73.0240	2010 Mw 8.8 Maule	Yes
40	Talcahuano	-36.7263	-73.1293	2010 Mw 8.8 Maule	Yes
41	Concepción	-36.8471	-73.0554	2010 Mw 8.8 Maule	Yes
42	Iloca	-35.0520	-72.1632	2010 Mw 8.8 Maule	Yes
43	San Pedro de La Paz	-36.8438	-73.1312	2010 Mw 8.8 Maule	No
44	Graneros	-34.0678	-70.7302	2010 Mw 8.8 Maule	No
45	Concepción	-36.8187	-73.0238	2010 Mw 8.8 Maule	Yes
46	San Pedro de La Paz	-36.8427	-73.1151	2010 Mw 8.8 Maule	No
47	Villarrica	-39.2921	-72.2134	2010 Mw 8.8 Maule	Marginal
48	La Serena	-29.9496	-71.2820	2015 Mw 8.3 Illapel	No
49	Chiguayante	-36.9011	-73.0300	2010 Mw 8.8 Maule	No
50	Concepción	-36.8228	-73.0449	2010 Mw 8.8 Maule	No
51	Curalinahue	-37.4739	-73.3437	2010 Mw 8.8 Maule	Marginal
52	Valdivia	-39.8140	-73.2459	2010 Mw 8.8 Maule	No
53	Concepción	-36.8376	-73.0618	2010 Mw 8.8 Maule	Yes
54	Talca	-35.4428	-71.6232	2010 Mw 8.8 Maule	Yes
55	Concepción	-36.8249	-73.0727	2010 Mw 8.8 Maule	No
56	Concepción	-36.8260	-73.0721	2010 Mw 8.8 Maule	No
57	Concepción	-36.8138	-73.0648	2010 Mw 8.8 Maule	No
58	Concepción	-36.8177	-73.0437	2010 Mw 8.8 Maule	No
59	Concepción	-36.8155	-73.0313	2010 Mw 8.8 Maule	No
60	Concepción	-36.8163	-73.0539	2010 Mw 8.8 Maule	No
61	Concepción	-36.8282	-73.0485	2010 Mw 8.8 Maule	No
62	Concepción	-36.8316	-73.0532	2010 Mw 8.8 Maule	No
63	Concepción	-36.8278	-73.0571	2010 Mw 8.8 Maule	No
64	Concepción	-36.8229	-73.0406	2010 Mw 8.8 Maule	No
65	Concepción	-36.8264	-73.0501	2010 Mw 8.8 Maule	No
66	Concepción	-36.8217	-73.0450	2010 Mw 8.8 Maule	No
67	Concepción	-36.8226	-73.0508	2010 Mw 8.8 Maule	No
68	Concepción	-36.8203	-73.0602	2010 Mw 8.8 Maule	No
69	Concepción	-36.8239	-73.0595	2010 Mw 8.8 Maule	No

Site_ID	City Location	Latitude	Longitude	Seismic Event	Surface Evidence of Liquefaction
70	Concepción	-36.8168	-73.0063	2010 Mw 8.8 Maule	Yes
71	Concepción	-36.7981	-73.0302	2010 Mw 8.8 Maule	Yes
72	Concepción	-36.7899	-73.0536	2010 Mw 8.8 Maule	Yes
73	Concepción	-36.8207	-73.0169	2010 Mw 8.8 Maule	Yes
74	Concepción	-36.8068	-73.0417	2010 Mw 8.8 Maule	Yes
75	Coihueco	-36.6372	-71.7975	2010 Mw 8.8 Maule	Yes
76	Curalinahue	-37.4732	-73.3482	2010 Mw 8.8 Maule	Yes
77	Talca	-35.1853	-71.7587	2010 Mw 8.8 Maule	Yes
78	Concepción	-36.8270	-73.0717	2010 Mw 8.8 Maule	Yes
79	San Pedro de La Paz	-36.8437	-73.1143	2010 Mw 8.8 Maule	Yes
80	Concepción	-36.8270	-73.0717	2010 Mw 8.8 Maule	No
81	Concepción	-36.7909	-73.0813	2010 Mw 8.8 Maule	No
82	Concepción	-36.8153	-73.0461	2010 Mw 8.8 Maule	No
83	La Serena	-29.9502	-71.2940	2015 Mw 8.3 Illapel	Yes
84	La Serena	-29.9536	-71.3013	2015 Mw 8.3 Illapel	Yes
85	Tongoy	-30.2603	-71.4811	2015 Mw 8.3 Illapel	Yes
86	Concepción	-36.8000	-73.0400	2010 Mw 8.8 Maule	Yes
87	Concepción	-36.8000	-73.0500	2010 Mw 8.8 Maule	Yes
88	San Pedro de La Paz	-36.8398	-73.1199	2010 Mw 8.8 Maule	Yes
89	Arauco	-37.2313	-73.4574	2010 Mw 8.8 Maule	Yes
90	Concepción	-36.8187	-73.0351	2010 Mw 8.8 Maule	No
91	Concepción	-36.8171	-73.0039	2010 Mw 8.8 Maule	No
100	Concepción	-36.8314	-73.0602	2010 Mw 8.8 Maule	No
101	Pichilemu	-34.4842	-72.0114	2010 Mw 8.8 Maule	Yes
102	Parral	-36.1972	-71.7350	2010 Mw 8.8 Maule	Yes
103	Talcahuano	-36.7295	-73.1436	2010 Mw 8.8 Maule	Yes
104	Dichato	-36.5504	-72.9361	2010 Mw 8.8 Maule	No
105	Dichato	-36.5389	-72.9261	2010 Mw 8.8 Maule	No
106	Tubul	-37.2247	-73.4707	2010 Mw 8.8 Maule	No
108	Arauco	-37.2494	-73.3349	2010 Mw 8.8 Maule	No
109	Arauco	-37.2564	-73.3164	2010 Mw 8.8 Maule	No
110	Llico	-37.2009	-73.5667	2010 Mw 8.8 Maule	No
111	Concepción	-36.8181	-73.0669	2010 Mw 8.8 Maule	Yes
112	Concepción	-36.8508	-73.0508	2010 Mw 8.8 Maule	Yes
113	Chiguayante	-36.8762	-73.0393	2010 Mw 8.8 Maule	Yes
114	Chiguayante	-36.8925	-73.0352	2010 Mw 8.8 Maule	Yes
115	Chiguayante	-36.9642	-73.0077	2010 Mw 8.8 Maule	Yes
116	Chiguayante	-36.9229	-73.0370	2010 Mw 8.8 Maule	Yes
117	Chiguayante	-36.9552	-73.0208	2010 Mw 8.8 Maule	Yes
118	Chiguayante	-36.9425	-73.0086	2010 Mw 8.8 Maule	Yes

Site_ID	City Location	Latitude	Longitude	Seismic Event	Surface Evidence of Liquefaction
119	Chiguayante	-36.9312	-73.0227	2010 Mw 8.8 Maule	No
120	Chiguayante	-36.9471	-73.0172	2010 Mw 8.8 Maule	No
121	Hualpén	-36.7760	-73.0936	2010 Mw 8.8 Maule	Yes
124	Coronel	-37.0146	-73.1484	2010 Mw 8.8 Maule	Yes
125	Concepción	-36.8153	-73.0808	2010 Mw 8.8 Maule	Yes
126	Los Ángeles	-37.4765	-72.3706	2010 Mw 8.8 Maule	Yes
127	Freire	-38.9771	-72.9820	2010 Mw 8.8 Maule	No
128	Hualpín	-39.0691	-73.1684	2010 Mw 8.8 Maule	No
129	Queule	-39.3630	-73.1803	2010 Mw 8.8 Maule	No
130	Angol	-37.7990	-72.7024	2010 Mw 8.8 Maule	Yes
131	Angol	-37.7974	-72.7052	2010 Mw 8.8 Maule	Yes
132	Purén	-38.0158	-73.0602	2010 Mw 8.8 Maule	Yes
133	Valdivia	-39.8230	-73.2321	2010 Mw 8.8 Maule	Yes
134	Valdivia	-39.8245	-73.2513	2010 Mw 8.8 Maule	Yes
135	Coñaripe	-39.5032	-72.1070	2010 Mw 8.8 Maule	Yes
136	Nirivilo	-35.5630	-72.1099	2010 Mw 8.8 Maule	Yes
137	Vichuquén	-34.8138	-72.0438	2010 Mw 8.8 Maule	Yes
138	Rarin	-34.7786	-71.9182	2010 Mw 8.8 Maule	Yes
139	Rio Claro	-35.2913	-71.2267	2010 Mw 8.8 Maule	Yes
140	Constitución	-35.3424	-72.4126	2010 Mw 8.8 Maule	Yes
141	Curepto	-35.0915	-72.0190	2010 Mw 8.8 Maule	Yes
142	Licantén	-34.9861	-72.0090	2010 Mw 8.8 Maule	Yes
143	Cocalán	-34.2074	-71.2763	2010 Mw 8.8 Maule	Yes
144	Ovalle	-30.9729	-71.6421	2015 Mw 8.3 Illapel	Yes
145	Curicó	-34.9758	-71.2295	2010 Mw 8.8 Maule	Yes
146	Curicó	-34.9696	-71.2581	2010 Mw 8.8 Maule	Yes
147	Penco	-36.7269	-72.9845	2010 Mw 8.8 Maule	Yes
148	Arauco	-37.2515	-73.3190	2010 Mw 8.8 Maule	No
149	Arauco	-37.2514	-73.3257	2010 Mw 8.8 Maule	Yes
150	Coronel	-36.9828	-73.1522	2010 Mw 8.8 Maule	Yes
151	Laja	-37.2778	-72.7079	2010 Mw 8.8 Maule	Yes
152	Hualpén	-36.7923	-73.0782	2010 Mw 8.8 Maule	Yes
153	Hualpén	-36.7909	-73.0813	2010 Mw 8.8 Maule	No
154	Concepción	-36.8187	-73.0633	2010 Mw 8.8 Maule	Yes
155	Concepción	-36.8448	-73.0559	2010 Mw 8.8 Maule	Yes
156	Arauco	-37.2432	-73.3091	2010 Mw 8.8 Maule	Yes
157	Concepción	-36.7900	-73.0548	2010 Mw 8.8 Maule	Yes
158	Concepción	-36.7913	-73.0576	2010 Mw 8.8 Maule	Yes
159	Concepción	-36.7892	-73.0522	2010 Mw 8.8 Maule	Yes
160	Concepción	-36.8167	-73.0062	2010 Mw 8.8 Maule	Yes

Site_ID	City Location	Latitude	Longitude	Seismic Event	Surface Evidence of Liquefaction
161	Concepción	-36.7978	-73.0304	2010 Mw 8.8 Maule	Yes
162	Concepción	-36.8207	-73.0171	2010 Mw 8.8 Maule	Yes
163	Concepción	-36.8189	-73.0151	2010 Mw 8.8 Maule	Yes
164	Concepción	-36.7939	-73.0331	2010 Mw 8.8 Maule	Yes
165	Temuco	-38.7240	-72.5990	2010 Mw 8.8 Maule	Yes
166	Concepción	-36.8282	-73.0426	2010 Mw 8.8 Maule	No
167	Concepción	-36.8249	-73.0399	2010 Mw 8.8 Maule	No
168	Concepción	-36.8287	-73.0504	2010 Mw 8.8 Maule	No
169	Concepción	-36.8327	-73.0505	2010 Mw 8.8 Maule	No
170	Concepción	-36.8308	-73.0441	2010 Mw 8.8 Maule	No
171	Concepción	-36.8218	-73.0365	2010 Mw 8.8 Maule	No
172	Concepción	-36.8227	-73.0419	2010 Mw 8.8 Maule	No
173	Concepción	-36.8233	-73.0409	2010 Mw 8.8 Maule	No
174	Concepción	-36.8204	-73.0413	2010 Mw 8.8 Maule	No
175	Paine	-33.8549	-70.7620	2010 Mw 8.8 Maule	Yes
176	San Antonio	-33.8288	-71.6437	2010 Mw 8.8 Maule	Yes
177	Valdivia	-39.8185	-73.2495	2010 Mw 8.8 Maule	Yes
178	Laraquete	-37.2065	-73.2113	2010 Mw 8.8 Maule	Yes
179	Arauco	-37.3070	-73.2650	2010 Mw 8.8 Maule	Yes
180	Cobquecura	-36.3864	-72.8340	2010 Mw 8.8 Maule	Yes
181	Santo Domingo	-33.6276	-71.6087	2010 Mw 8.8 Maule	Marginal
182	Laraquete	-37.1690	-73.1878	2010 Mw 8.8 Maule	Yes
183	Talcahuano	-36.7738	-73.1130	2010 Mw 8.8 Maule	No
184	Corral	-39.9492	-73.3127	2010 Mw 8.8 Maule	Yes
185	Llico	-34.7747	-72.0612	2010 Mw 8.8 Maule	Yes
186	Chonchi	-42.6892	-73.9409	2016 Mw 7.6 Melinka	Yes
187	Puahun	-36.3826	-72.8126	2010 Mw 8.8 Maule	Yes
188	San Pedro de La Paz	-36.8449	-73.1125	2010 Mw 8.8 Maule	Yes
189	Talcahuano	-36.7755	-73.0778	2010 Mw 8.8 Maule	Yes
190	Talcahuano	-36.7455	-73.0841	2010 Mw 8.8 Maule	Yes
191	La Serena	-29.9045	-71.2609	2015 Mw 8.3 Illapel	No
192	Lebu	-37.6044	-73.6536	2010 Mw 8.8 Maule	Yes
193	Concepción	-36.8448	-73.0499	2010 Mw 8.8 Maule	No
194	Talcahuano	-36.7070	-73.1134	2010 Mw 8.8 Maule	Yes
195	La Serena	-29.9262	-71.2778	2015 Mw 8.3 Illapel	No
196	Concepción	-36.8125	-73.0690	2010 Mw 8.8 Maule	Yes
197	Valparaiso	-33.0374	-71.6273	2010 Mw 8.8 Maule	Yes
198	Concepción	-36.8270	-73.0717	2010 Mw 8.8 Maule	Yes
199	San Pedro de La Paz	-36.8462	-73.1164	2010 Mw 8.8 Maule	Yes
200	Santa Juana	-36.8517	-73.0728	2010 Mw 8.8 Maule	Yes

Site_ID	City Location	Latitude	Longitude	Seismic Event	Surface Evidence of Liquefaction
201	Viña del Mar	-33.0359	-71.5271	2010 Mw 8.8 Maule	No
202	Viña del Mar	-33.0375	-71.5223	2010 Mw 8.8 Maule	No
203	Viña del Mar	-33.0262	-71.5552	2010 Mw 8.8 Maule	No
204	Viña del Mar	-33.0292	-71.5426	2010 Mw 8.8 Maule	No
205	San Pedro de La Paz	-36.8326	-73.1088	2010 Mw 8.8 Maule	No
206	San Pedro de La Paz	-36.8415	-73.1037	2010 Mw 8.8 Maule	No
207	Chiguayante	-36.9245	-73.0216	2010 Mw 8.8 Maule	No
208	Puqueldón	-43.0849	-73.7136	2016 Mw 7.6 Melinka	Yes
209	Quellón	-43.1094	-73.6271	2016 Mw 7.6 Melinka	Yes
210	Chonchi	-42.6526	-74.1169	2016 Mw 7.6 Melinka	Yes
211	Quellón	-42.9074	-73.7013	2016 Mw 7.6 Melinka	Yes
212	Puqueldón	-42.6680	-73.5829	2016 Mw 7.6 Melinka	Yes
213	Chonchi	-42.6683	-73.9972	2016 Mw 7.6 Melinka	Yes
214	Quellón	-43.3595	-74.1315	2016 Mw 7.6 Melinka	Yes
215	Queilen	-42.8228	-73.6212	2016 Mw 7.6 Melinka	Yes
216	Queilen	-42.8752	-73.5718	2016 Mw 7.6 Melinka	Yes
217	Queilen	-42.8647	-73.5822	2016 Mw 7.6 Melinka	Yes
218	Camarones	-19.0078	-70.0025	2014 Mw 8.2 Iquique	Yes
219	Huara	-19.5520	-69.9409	2014 Mw 8.2 Iquique	No
220	Huara	-19.4545	-69.9468	2014 Mw 8.2 Iquique	Yes

3.6 Surface Geology

It has been recognized that liquefaction resistance of sand increases with age due to processes such as cementation at particle contacts and increasing frictional resistance resulting from particle rearrangement and interlocking. The soils derived from the Holocene (deposited during the last 10,000 years) are the most susceptible to liquefaction. These soils are weak and non-cohesive, so they have a greater probability of liquefying compared to old soils. Youd and Hoose (1977) stated that as a general rule, alluvial deposits older than the late Pleistocene (10,000-130,000 years) are unlikely to liquefy except under severe seismic loading conditions.

Young soils are generally found on riverbanks, beaches, dunes, and areas where sand and sediment were accumulated by wind or water transport. From this, the surface geological age of the sites was incorporated into the database.

3.7 Geotechnical Tests

After the compilation of the case history data, the database was expanded with data from geotechnical tests, including SPT tests, CPT tests, and geophysical measurements. The available information from the geotechnical tests is shown in Table 3.

Table 3 Available information from geotechnical tests

Test	Available Information					
	SPT, Vs and f0	**SPT and Vs**	**SPT**	**Vs and f0**	**Vs**	**CPT**
# Total of Sites	60	54	9	23	19	15

3.7.1 Borehole Information

The database contains geotechnical information from boreholes such as SPT data, CPT data, groundwater table depth and laboratory test data. The execution time of the SPT and CPT tests in relation to seismic events is not clear in all cases. However, most of the boreholes were realized after Maule 2010. This data was obtained through reports of soil mechanics from the Ministry of Public Works (MOP), the associated company R&V Engineers and the fieldwork of the University of Concepción.

SPT data includes a total of 312 SPT tests and 26 CPT tests, with varying depths between 5.0 and 72.0 m. Also, includes tables with the latitude and longitude of the test, groundwater table depth, hammer energy, bar diameter and soil layers.

3.7.2 Geophysical Measurements

The database includes geophysical test data obtained from geophysical reports. In the case of sites where geophysical reports were not available, the information was acquired through non-invasive methods, using passive and active sources. Environmental noise measurements (passive source) were recorded with Tromino® instruments. The environmental noise was

processed using the SPAC technique (Spatial Autocorrelation (Aki, 1957)) using the vertical component, mainly composed of Rayleigh-type waves. The source measurements were recorded using a hammer blow to the ground as the source. The method used to obtain the dispersion curve was the frequency-wave number analysis (F-K; (Lacoss, Kelly, & Toksoz, 1969); (Kvaerna & Ringdahl, 1986)).

From the autocorrelation curves obtained from SPAC and the dispersion curve obtained with F-K, the shear wave velocity profiles were obtained through the inversion of the dispersion curve. It is important to indicate that the inversion procedure is non-unique and different dispersion curves may provide different velocity profiles (Foti, Hollender, & Garofalo, 2018). Finally, the predominant frequency (f_0) and amplitude (A_0) were obtained from the results of the HVSR curves.

The geophysical test data includes a total of 203 shear wave velocities measurements and 243 predominant frequency curves. Also, incorporate tables with latitude and longitude of the test, duration of the records and if is a clear peak (yes or no).

3.8 Seismic Parameters

The seismic events were recorded by ground motion stations and GPS stations operated by the National Seismological Center (2018) and other local networks. The hypocenter locations (i.e., latitude, longitude, and depth) are the coordinates reported by CSN, also centroid and moment tensor are reported by Global CMT project (Ekström, Nettles, & Dziewonski, 2012). The source-to-site distance measures included are the closest distance to the earthquake rupture plane (Rrup), epicentral distance (Repi), and hypocentral (Rhyp) distances. The finite fault solutions for these events are compiled by SRCMOD database (Mai & Thingbaijam, 2014).

3.9 Intensity Measures

An important part of seismic behavior of soil is cyclic demand. Unfortunate, seismic intensities of case history data nearby to strong ground motion stations are lack. Consequently, the estimation of seismic intensities at case history is based on ground motion prediction models (GMPM) available for Chilean subduction zone (Montalva, Bastías, & Rodríguez-Marek, 2017). The ground motion intensity measures (IM) included in the database are the peak ground acceleration (PGA) and velocity (PGV), and the spectral responses: PSA and SV in the predominant frequency of the soil, PSA and SV in 1 and 0.2 seconds. PSA and SV estimation corresponds to geometric mean of the horizontal components of the ground motion.

Typically, error of GMPM is split in several components (Al Atik, et al., 2010): site term, event term, and residual error. This variability could be used to fix the median estimation of intensity at specific event or site. Due to between-event residuals are available for the originals GMPMs, intensities measures corrected and not-corrected by event-term are computed and reported in dataset.

3.10 Conclusion

The structure of the database was presented as well as the historical performance (surface evidence of liquefaction) of the case-history data, to finally explain the geotechnical and seismic properties incorporated in the database.

CHAPTER 4 RESULTS

4.1 Introduction

This chapter shows the results obtained from the geotechnical and seismic properties incorporated in the database. A qualitative and quantitative analysis of the parameters involved in the phenomenon is included.

4.2 Geotechnical Tests

4.2.1 Borehole Information

The database contains geotechnical information from boreholes such as SPT data, CPT data, groundwater table depth and laboratory test data. The execution time of the SPT and CPT tests in relation to seismic events is not clear in all cases. However, most of the boreholes were realized after Maule 2010.

SPT data includes a total of 312 SPT tests and 26 CPT tests, with varying depths between 5.0 and 72.0 m. A summary of the borehole depth and ground water table depth for all SPT tests compiled is shown in Table 4. Figure 7 shows the variability of the borehole depths, where the major number of boreholes is between 25 and 35 m deep. Besides, the ground water table depth is generally minor than 3 m.

Table 4 SPT boreholes data from cases histories

Surface Liquefaction Evidence	#SPT Total Boreholes	Borehole Depth (m)		Water Table Depth (m)	
		Min	Max	Min	Max
Yes	204	5.0	50.0	0.1	12.0
No	100	6.3	53.7	0.3	8.5
Marginal	8	6.0	46.0	0.7	4.4

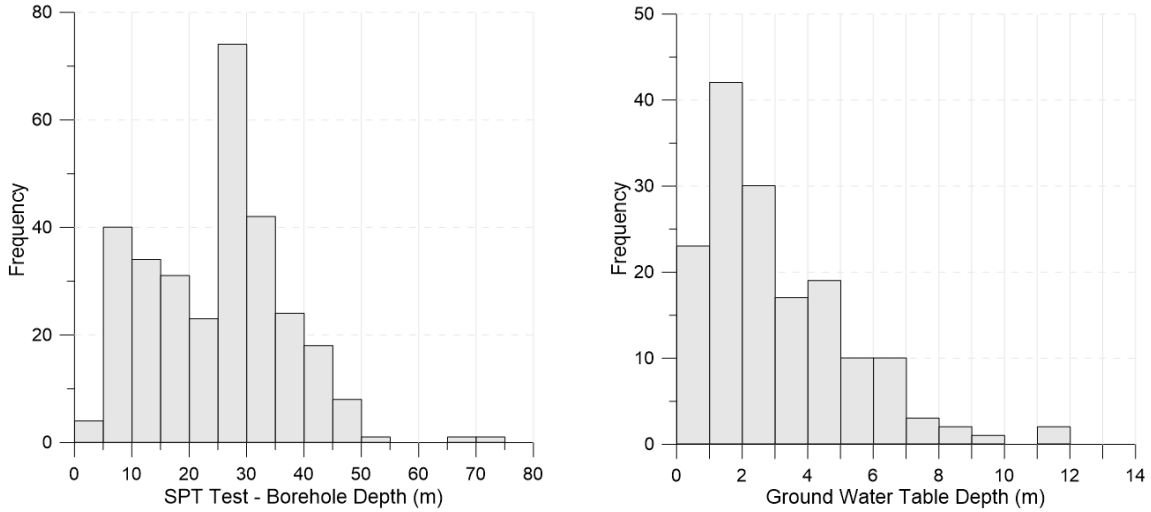

Figure 7. Histograms of borehole depth and ground water table depth for all SPT tests compiled in the curated dataset.

The soil layer tables contain SPT blow count (N_m), and laboratory test data from samples obtained in the boreholes. Figure 8 shows a histogram of SPT Nm values and sand content for depths less than or equal to 15 m. One of the most important characteristics of the database is the great variability of information it provides with SPT N_m values between 2.0 and 100. In addition, database contains more than 2300 samples for depths less than or equal to 15 m, with sand contents from 0 to 100% in all case histories, which vary from poorly graded sands (SP in the USCS system), to silts of high plasticity and clays of low plasticity (MH-ML-CL).

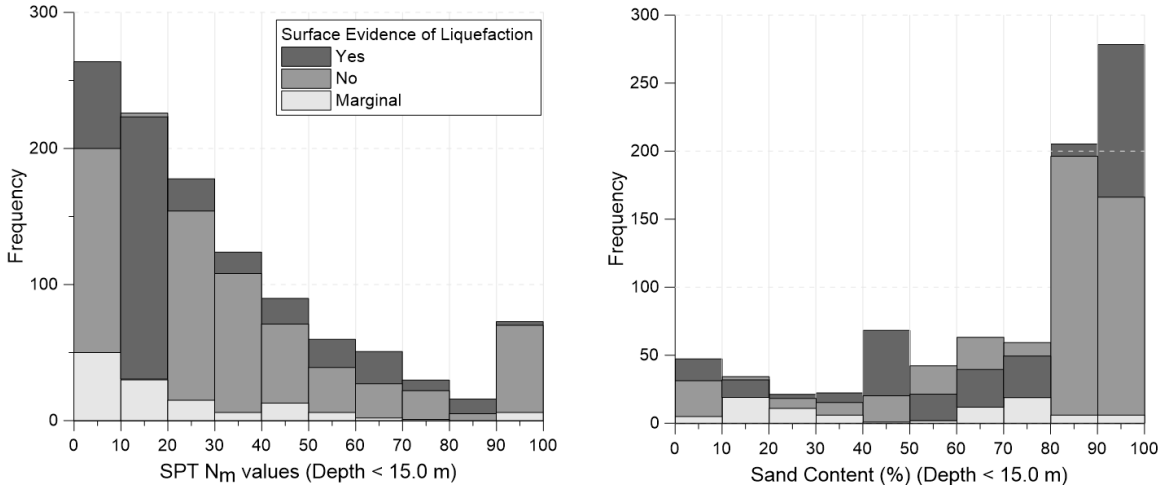

Figure 8. Histograms of SPT Nm values and sand content for depths less than or equal to 15 m

A density plot of the SPT samples depth vs distance (Rrup or Rhyp) is shown in Figure 9. Then, Figure 10 shows the SPT Nm values for all the samples that compose the database. It is important to indicate that depths of Figure 10 correspond to the samples for the case histories and are not associated with the phenomenon of liquefaction at that depth. This database does not calculate or evaluate the liquefaction triggering in soils but provides data to train or evaluate predictive liquefaction models.

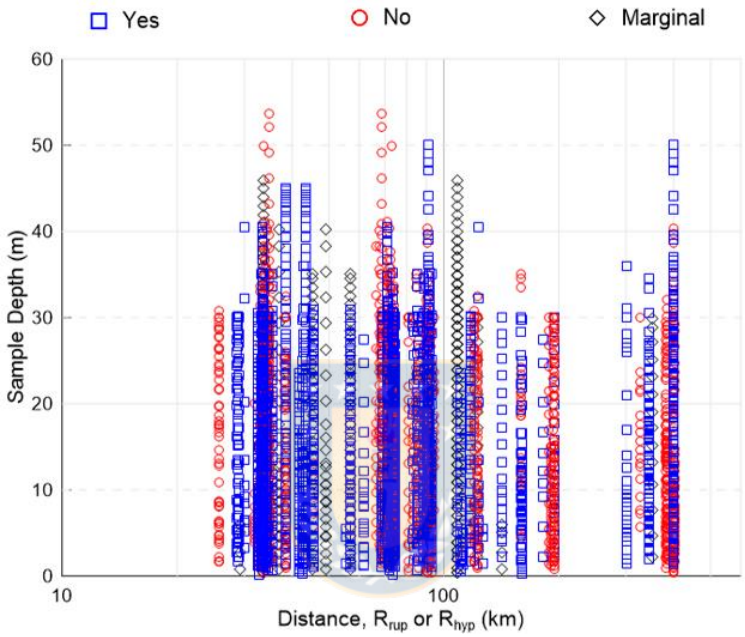

Figure 9. Density plot of SPT samples depth vs distance, Rrup or Rhyp. The blue squares are samples of liquefaction case histories, the red pots are samples of non-liquefaction case histories, and black diamonds are samples of marginal case histories.

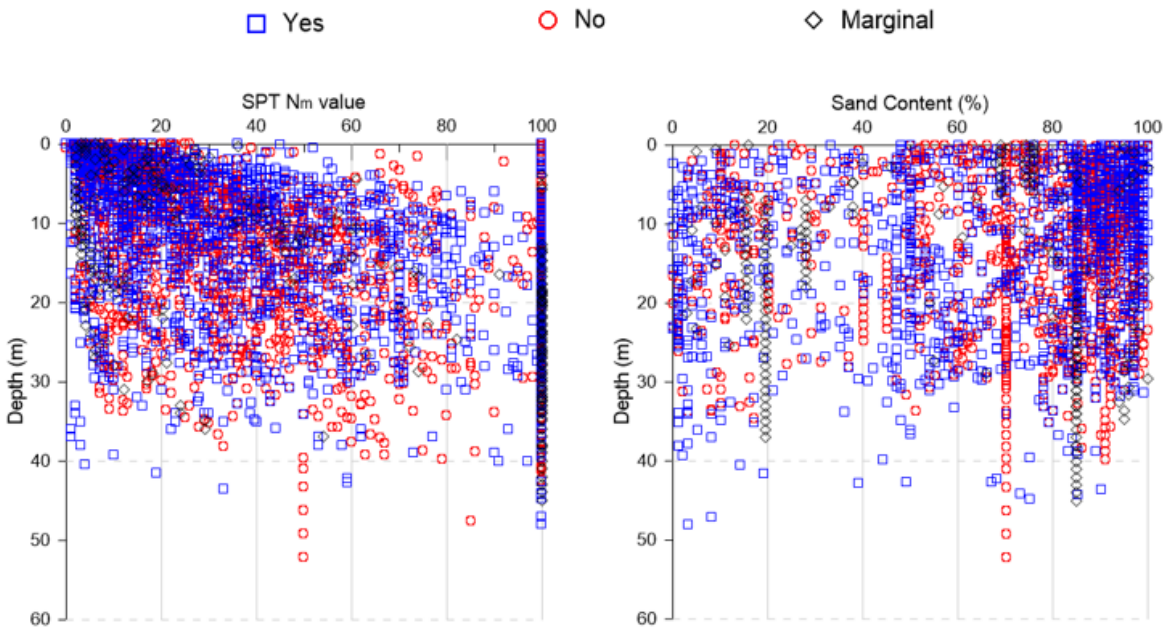

Figure 10. Density plots with the depth of the sample versus the SPT Nm value and sand content. Left: sample depth vs SPT Nm value; right: sample depth vs sand content. The blue squares are samples of liquefaction case histories, the red pots are samples of non-liquefaction case histories, and black diamonds are samples of marginal case histories.

4.2.2 Geophysical Measurements

The geophysical test data includes a total of 213 shear wave velocities measurements and 243 predominant frequency curves. A summary of the geophysical test data is shown in Table 5 and Table 6.

Table 5 Shear wave velocities from cases histories

Surface Liquefaction Evidence	#Vs Total Measuraments	V_{s30} (m/s)		V_{s18} (m/s)	
		Min	Max	Min	Max
Yes	109	128.6	635.0	154.9	889.1
No	98	130.1	852.4	150.4	1024.2
Marginal	6	156.4	400.7	172.9	402.8

Table 6 HVSR curves data from cases histories

Surface Liquefaction Evidence	#f0 Total Measuraments	HVSR Curves				Predominant Period of Sites (sec)	
		Predominant Frequency (Hz)		Predominant Amplitude (sec)			
		Min	Max	Min	Max	Min	Max
Yes	115	0.42	5.06	1.09	18.12	0.20	2.20
No	108	0.57	8.91	1.76	12.58	0.15	1.71
Marginal	20	0.41	3.34	3.52	9.66	0.22	2.31

Figure 11 shows the variability of average shear wave velocity for 30 m depth (Vs,30) and predominant period for all case histories compiled in the database. From the Vs, 30 results it can be observed that the major number of sites have vs, 30 less than 350 m/s, which corresponds to the range from dense or firm soils to soils of compactness or medium consistency.

Figure 12 shows the predominant frequencies and amplitudes obtained from the results of the HVSR curves, which maximum and minimum values are in Table 6.

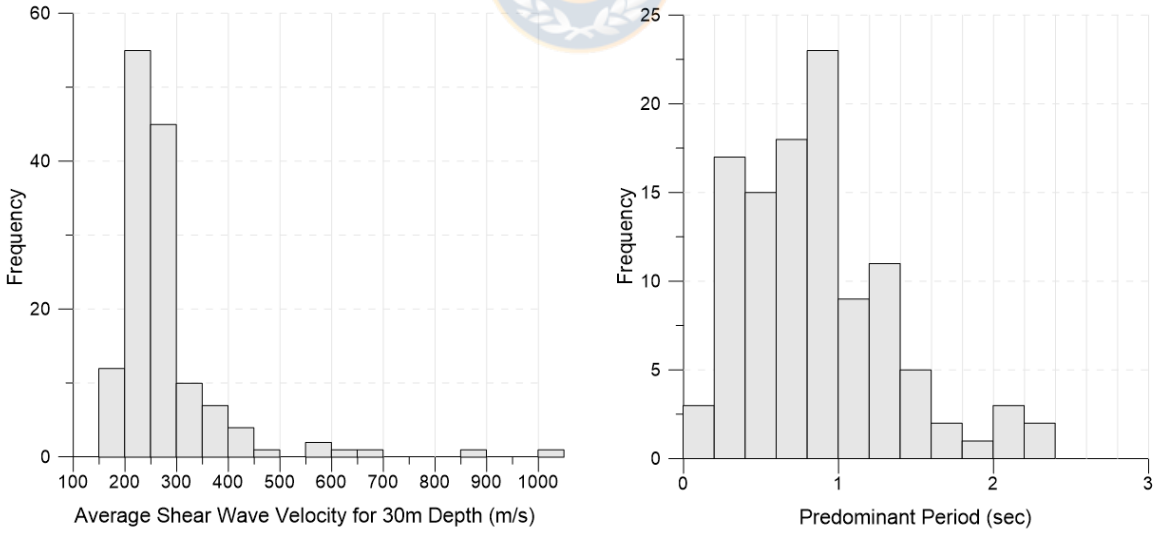

Figure 11. Histograms of average shear wave velocity for 30 m depth and predominant period for all case histories compiled in the database.

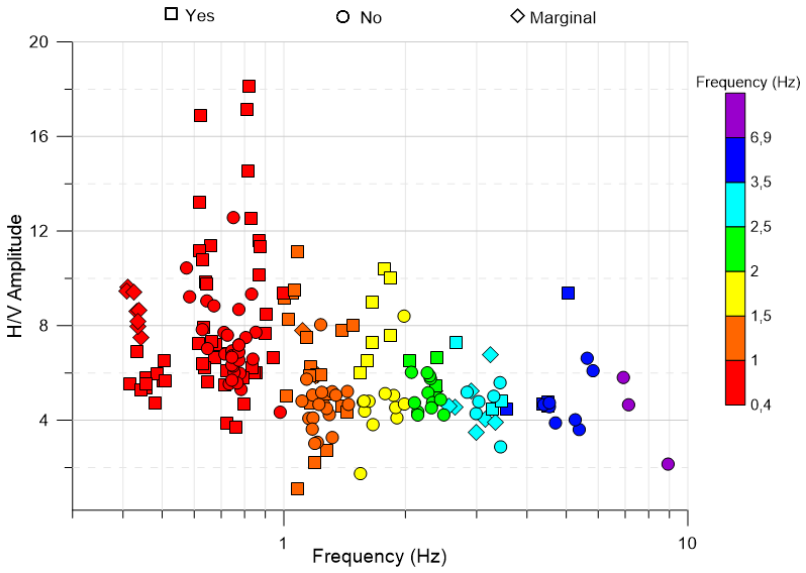

Figure 12. Plot of predominant frequencies and amplitudes obtained from the results of the HVSR curves. The squares are H/V of liquefaction case histories, the pots are H/V of non-liquefaction case histories, and diamonds are H/V of marginal case histories.

4.3 Seismic Parameters

4.3.1 Seismic Events

The source-to-site distance measures included are the closest distance to the earthquake rupture plane (Rrup), epicentral distance (Repi), and hypocentral (Rhyp) distances. A summary of the source-to-site distances data is shown in Table 7. Figure 13 shows the variability of Repi and Rrup, for all case histories compiled in the database.

Table 7 Source-to-site distances data of cases histories

Surface Evidence of Liquefaction	Repi (km)		Rhyp (km)		Rrup (km)	
	Min	Max	Min	Max	Min	Max
Yes	35.69	414.12	43.57	414.87	25.22	103.16
No	150.36	401.30	0.58	402.08	61.70	94.39
Marginal	42.08	351.33	48.94	352.21	29.17	122.04

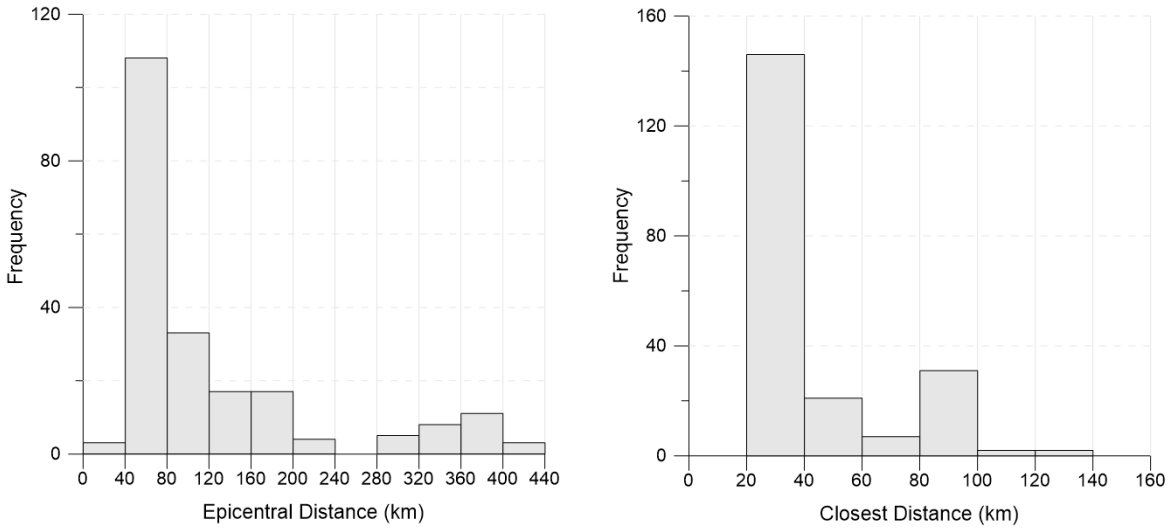

Figure 13. Histograms of the epicentral distance (Repi) and closest distance to the earthquake rupture plane (Rrup), for all case histories compiled in the database.

4.3.2 Intensity Measures

The ground motion intensity measures (IM) included in the database are the peak ground acceleration (PGA) and velocity (PGV), and the spectral responses: PSA and SV in the predominant frequency of the soil, PSA and SV in 1 and 0.2 seconds. PSA and SV estimation corresponds to geometric mean of the horizontal components of the ground motion. A summary of the intensity measures is show in Table 8 and a plots are shown from Figure 14 to Figure 15.

Table 8 Intensity measures of cases histories

Surface Evidence of Liquefaction	PGA (g)		PGV (cm/s)		Sa at 1 sec (g)	
	Min	Max	Min	Max	Min	Max
Yes	0.16	0.45	16.13	75.26	0.15	0.63
No	0.17	0.43	14.94	73.75	0.00	0.62
Marginal	0.14	0.46	33.33	67.51	0.22	0.57

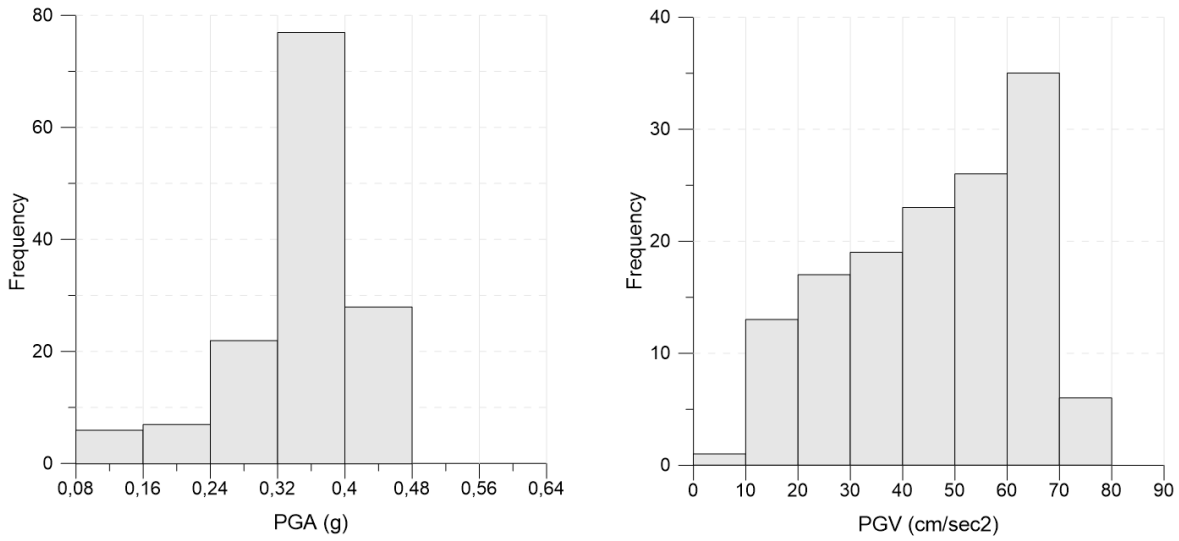

Figure 14. Histograms of peak ground acceleration (PGA) and peak ground velocity (PGV) for all case histories compiled in the database.

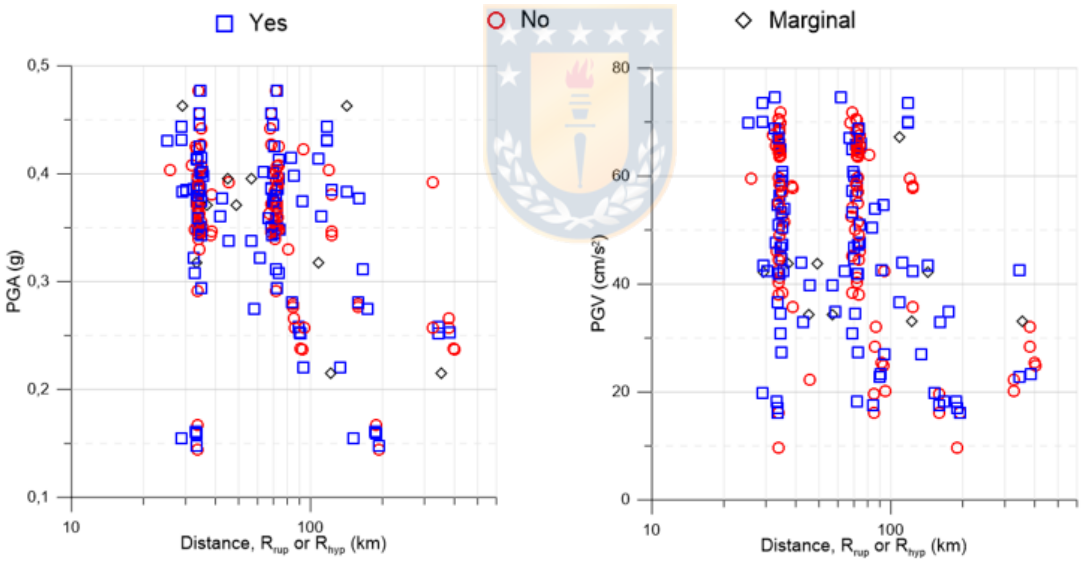

Figure 15. Density plot of peak ground acceleration (PGA) and velocity (PGV) vs distance Rhyp, Rrup, or Repi. The blue squares are liquefaction sites, the red pots are of non-liquefaction sites, and black diamonds are marginal sites.

CHAPTER 5 CONCLUSIONS AND DISCUSSION

The database developed in this research is the most extensive published to date in the national zone and includes 209 case histories compiled from the most important earthquakes of the last time, 2010 Mw 8.8 Maule, 2014 Mw 8.2 Iquique, 2015 Mw 8.3 Illapel and 2016 Mw 7.6 Melinka. The data associated with this article are available in DesignSafe (https: // XXXXX), where users can freely download and process data.

This research included a description of the database structure, followed by the historical performance (surface evidence), geotechnical, geophysical and laboratory test data, earthquake information and ground motion intensity measures. The compiled, post-processed data allows researchers to easily access and analyze the geotechnical properties of soils, to characterize the seismic demand and the soil response.

The information gathered and reported in this database should serve as a tool to training or testing of new and existing liquefaction-prediction models. Prior to such analyses, users should carefully consider the limitations and uncertainties of the data compiled. To continue improving the liquefaction prediction models, the database must continue to grow, especially the intensity measures. Outstanding authors in soil liquefaction indicate that studies and practices have increasingly shown that Peak ground acceleration (PGA) and Peak ground velocity (PGV) parameters are not necessarily linearly correlated with the seismic frequency distribution, duration and influence of the damage. Therefore, PGA and PGV data may not indicate the wave frequency components of the earthquake or its duration. (EPRI, 1988). Furthermore, practical experience indicates that a prolonged vibration cycle is the key factor in structural damage for various seismic disasters, so it is necessary to incorporate the duration of ground movement (Pathak & Dalvi, 2013).

The American Electric Power Research Institute (EPRI) proposes the concept of accumulated ground velocity (CAV). CAV includes the cumulative effects of the duration of ground movement. This is a key advantage of CAV over peak response parameters and is one of the reasons why EPRI (1988) found it to be the instrument intensity measure that best correlated with the structural damage (Campbell & Borzognia, 2010).

Kramer and Mitchell (2006)recommend the use of a filtered variant of CAV, which they call CAV5 to replace PGA and magnitude in the evaluation of liquefaction potential. In this way, they propose the use of a new intensity measure (MI), with the expectation that when combined with one or more structural MIs, an MI vector can be formed, which will be useful to predict the performance of the structure systems of the soil, which include liquefiable soils.

CHAPTER 6 REFERENCES

Aki, K. (1957). *Space and Time Spectra of Stationary Stochastic Waves with Special Reference to Microtremors.* Tokyo University.

Al Atik, L., Abrahamson, N., Bommer, J., Scherbaum, F., Cotton, F., & Kuehn, N. (2010). The Variability of Ground-Motion Prediction Models and Its Components. *Seismological Research Letters, 81*(5), 794–801. doi:10.1785/gssrl.81.5.794

Alfaro, F. (2013). *Comparación entra la Metodología para evaluar el Potencial de Riesgo de Licuación y los Catastros Realizados luego del Terremoto de 2010 en Concepción.* Universidad del Bio Bío, Departamento de Ingeniería Civil y Ambiental, Concepción.

Andrus, R., & Stokoe, K. (2000). Liquefaction Resistance of Soils from Shear-Wave Velocity. *Journal of Geotechnical and Geoenvironmental Engineering, 126*(11). doi:10.1061/(ASCE)1090-0241(2000)126:11(1015).

Barrientos, S., & National Seismological Center (CSN). (2018, March/April). The Seismic Network of Chile. *Seismological Research Letters, 89*(2A). doi:10.1785/0220160195

Bastías, N., Montalva, G., & Leyton, F. (2018). Modelo Predictivo de Velocidad Máxima (PGV) y Espectral (PSv) para Zona de Subducción Chilena. *X Congreso SOCHIGE.* Valparaiso.

Boulanger, R., & Idriss, I. (2014). *CPT and SPT Based Liquefaction Triggering Procedures.* University of California , Department of Civil and Environmental Engineering, Davis, California .

Boulanger, R., & Idriss, I. (2016). CPT-Based Liquefaction Triggering Procedure. *Journal of Geotechnical and Geoenvironmental Engineering, 142*(2). doi:10.1061/(ASCE)GT.1943-5606.0001388

Brandenberg, S., Zimmaro, P., & Stewart, J. (2020). Next-Generation Liquefaction Database. *Earthquake Spectra, 36*(2), 939-959. doi:10.1177/8755293020902477

Campbell, K., & Borzognia, Y. (2010). A Ground Motion Prediction Equation for the Horizontal Component of Cumulative Absolute Velocity (CAV) Based on the PEER-NGA Strong Motion Database. *Earthquake Spectra, 26*(3), 635-650.

Cetin, K., Seed, R., Der Kiureghian, A., Tokim, K., Harder Jr, L., Kayen, R., & Moss, R. (2004). Standard Penetration Test-Based Probabilistic and Deterministic Assessment of Seismic Soil Liquefaction Potential. *Journal of Geotechnical and Geoenvironmental Engineering, 130*(12), 1314-1340. doi:10.1061/(ASCE)1090-0241(2004)130:12(1314)

Cetin, K., Seed, R., Kayen , R., Moss, R., Bilge, H., Ilgac, M., & Chowdhury, K. (2018). Dataset on SPT-Based Seismic Soil Liquefaction. *Data in Brief, 20*, 544-548. doi:10.1016/j.dib.2018.08.043

Contreras, J. (2012). *Estudio de los Efectos del Terremoto del 27/2/2010 en la Zona de las Comunas de Buín y Paine de la Región Metropolitana.* Universidad de Chile, Departamento de Ingeniería Civil, Santiago.

Dobry, R., & Abdoun, T. (2015). Threshold Load Factor for Liquefaction Triggering Evaluations. *Journal of Geotechnical and Geoenvironmental Engineering, 141*(02815003). doi:10.1061/(ASCE)GT.1943-5606.0001399

Dobry, R., Ladd, R., Yokel, F., Chung, R., & Powell, D. (1982). *Prediction of Pore Water Pressure Buildup and Liquefaction of Sand by the Cyclic Strain Method* (Vol. 138). Washington DC.

Ekström, G., Nettles, G., & Dziewonski, A. (2012). The Global CMT Project 2004-2010: Centroid-Moment Tensors for 13,017 Earthquakes. *Physics of The Earth and Planetary Interiors, 200-201*, 1-9. doi:10.1016/j.pepi.2012.04.002

EPRI. (1988). *A Criterion for Determining Exceedance of the Operating Basis Earthquake,*. Palo Alto, California: Report No.EPRI NP-5930.

Espinoza, D. (2018). *Evaluación del Potencial de Licuación en Zonas de Subducción.* Universidad de Concepción, Departamento de Ingeniería Civil, Concepción.

FHWA. (2011). *Postearthquake Reconnaissance Report on Transportation Infrastructure Impact of the February 27, 2010, Offshore Maule Earthquake in Chile.* US Department of Transportation.

Foti, S., Hollender, F., & Garofalo, F. (2018). Guidelines for the Good Practice of Surface Wave Analysis: A Product Of The Interpacific Project. *Bulletin of Earthquake Engineering, 16*, 2367-2420.

GEER. (2010). *Geo-Engineering Reconnaissance of the 2010 Maule, Chile Earthquake.* Geotechnical Extreme Events Reconnaissance. Report No. GEER-022. doi:10.18118/G6NP4W

GEER. (2010). *Geo-Engineering Reconnaissance of the 2010 Maule, Chile Earthquake.* Geotechnical Extreme Events Reconnaissance Association. Report No. GEER-022. doi:10.18118/G6NP4W

GEER. (2014). *Geotechnical aspects of April 1, 2014 M8.2 Iquique, Chile earthquake.* Geotechnical Extreme Events Reconnaissance Association. Report No. GEER-038. doi:10.18118/G6KS3X

GEER. (2015). *Geotechnical Reconnaissance of the 2015 Mw8.3 Illapel, Chile Earthquake.* Geotechnical Extreme Events Reconnaissance Association. Report No. GEER-043. doi:10.18118/G6NP4W

González, J. (2015). *Estudio del Fenómeno de Licuación en Chile para el Terremoto del Maule 2010.* Universidad de Chile, Departamento de Ingeniería Civil, Santiago.

González, J., & Verdugo, R. (2014). *Sitios Afectados por Licuefacción a Causa del Terremoto 27-F.* Sociedad Chilena de Geotecnia.

Idriss, I., & Boulanger, R. (2008). *Soil Liquefaction During Earthquakes.* Earthquake Engineering Research Institute, Oakland, California.

Idriss, I., & Boulanger, R. (2010). *SPT-Based Liquefaction Triggering Procedures.* College of Engineering, Departament of Civil & Environmental Engineering. Davis, California: University of California .

Ishihara, K. (1996). *Soil Behaviour in Earthquake Geotechnics.* Oxford University Press Inc, New York.

Kayen, R., Moss, R., Thompson, E., Seed, R., Cetin, K., Der Kiureghian, A., . . . Tokimatsu, K. (2013). Shear-Wave Velocity-Based Probabilistic and Deterministic Assessment of Seismic Soil Liquefaction Potential. *Journal of Geotechnical and Geoenvironmental Engineering, 139*, 407-419. doi:10.1061/(ASCE)GT.1943-5606.0000743

Kramer, S. (1996). *Geotechnical Earthquake Engineering.* Prentice Hall, Upper Saddle River.

Kramer, S., & Mitchell, R. (2006). Ground Motion Intensity Measures For Liquefaction Hazard Evaluation. *Earthquake Spectra, 22*(2), 413-438.

Kvaerna, T., & Ringdahl, F. (1986). Stability of Various FK-Estimation Techniques, in Semiannual Technical Summary, 1 October 1985 - 31 March 1986. *In NORSAR Scienti. Report, 1-86/87*, 29-40.

Lacoss, R., Kelly, E., & Toksoz, M. (1969). Estimation of Seismic Noise Structure Using Arrays. *Geophysics, 34*, 21-38.

Ladd, R. (1978). Preparing Test Specimens Using Undercompaction. *Geotechnical Testing Journal, 1*(1), 16-23.

Mai , P., & Thingbaijam, K. (2014). SRCMOD: An Online Database of Finite-Fault Rupture Models. *Seismological Research Letters, 85*(6), 1348-1357.

Montalva, G., & Leyton, F. (2014). Discussion to: "Shear-Wave Velocity-Based Probabilistic And Deterministic Assessment of Seismic Soil Liquefaction Potential. *Journal of Geotechnical and Geoenvironmental Engineering , 140*(4), 407-419.

Montalva, G., & Ruz, F. (2017). Liquefaction Evidence in the Chilean Subduction Zone. *PDB-III Earthquake Geotechnical Engineering.* Vancouver, Cánada.

Montalva, G., Bastías, N., & Rodríguez-Marek, A. (2017). *Ground Motion Prediction Equation for the Chilean Subduction Zone.* Bulletin of the Seismological Society of America. doi:10.1785/0120160221

Pastén, C., Campos, F., Ochoa-Cornejo, F., Ruiz, S., Valdebenito, G., Alvarado, D., . . . Moffat, R. (2021). The Role of Site Conditions on the Structural Damage in the City of Valdivia during the 22 May 1960 Mw 9.5 Megathrust Chile Earthquake. *Seismological Research Letters*. doi:10.1785/0220190321

Pathak, S., & Dalvi, A. (2013). Elementary Empirical Liquefaction Model. *Journal of the International Society for the Prevention and Mitigation of Natural Hazards, 69*, 425-440. doi:10.1007/s11069-013-0723-x

Roncagliolo, J. (2017). *Evaluación De Potencial De Licuación De Suelos En Zona Subductiva Chilena.* Universidad de Concepción, Departamento de Ingeniería Civil, Concepción.

Seed, H., & Idriss, I. (1971). Simplified Procedure for Evaluating Soil Liquefaction Potential. *Journal of the Soil Mechanics and Foundations Division Proceedings of the American Society of Civil Engineers*.

Seed, H., Idriss, I., & Arango, I. (1983). Evaluation of Liquefaction Potential Using Field Performance Data. *Journal of Geotechnical & Geoenvironmental Engineering, 109*(3), 458–482.

Sernageomin. (2010). *Efectos geológicos del sismo del 27 de Febrero del 2010.* Servicio Nacional de Geología y Minería.

Sernageomin. (2017). *Efectos Geológicos del Terremoto de Chiloé del 25 de Diciembre de 2016 Región de Los Lagos.* Servicio Nacional de Geología y Minería.

Yasuda, S., Verdugo, R., Konagai, K., Sugano, K., Villalobos, F., Okamura, M., . . . Towhata, I. (2010). Description and Analysis of Geotechnical Aspects Associated to the 2010 Chile Earthquake. *ISSMGE Bulletin, 4*(2), 16-27.

Youd, T., & Hoose, S. (1977). Liquefaction susceptibility and Geologic Setting. *Sixth World Conference on Earthquake Engineering, Volume 3.* New Jersey.

Youd, T., Idriss, I., Andrus, R., Arango, I., Castro, G., Christian , J., . . . Marcuson, W. (2001). Liquefaction Resistance of Soils: Summary Report from the 1996 NCEER and 1998 NCEER/NSF Workshops on Evaluation of Liquefaction Resistance of Soils. *Journal of Geotechnical and Geoenvironmental Engineering, 127*. doi:10.1061/(ASCE)1090-0241(2001)127:10(817).